ORIGINAL RESEARCH

Multi-Site Benchmark Study for Standardized Relative Cerebral Blood Volume in Untreated Brain Metastases Using the DSC-MRI Consensus Acquisition Protocol

Sarah Kohn Loizzo, Melissa A. Prah, Min J. Kong, Daniel Phung, Javier C. Urcuyo, Jason Ye, Frank J Attenello, Jesse Mendoza, Yuxiang Zhou, Mark S. Shiroishi, Leland S. Hu, Kathleen M. Schmainda

ABSTRACT

BACKGROUND AND PURPOSE: A national consensus recommendation for the collection of DSC (dynamic susceptibility contrast) MRI perfusion data, used to create maps of relative cerebral blood volume (rCBV), has been recently established for primary and metastatic brain tumors. The goal was to reduce inter-site variability and improve ease of comparison across time and sites, fostering widespread use of this informative measure. To translate this goal into practice the prospective collection of consensus DSC-MRI data and characterization of derived rCBV maps in brain metastases is needed. The purpose of this multi-site study was to determine rCBV in untreated brain metastases in comparison to glioblastoma and normal appearing brain using the national consensus protocol.

MATERIALS AND METHODS: Subjects from three sites with untreated enhancing brain metastases underwent DSC-MRI according to a recommended option that uses a mid-range flip angle, GRE-EPI acquisition and the administration of both a pre-load and 2nd DSC-MRI dose of 0.1 mmol/kg GBCA. Quantitative maps of standardized rCBV (sRCBV) were generated and enhancing lesion ROIs determined from post-contrast T1-weighted images alone or calibrated difference maps, termed delta T1 (dT1) maps. Mean sRCBV for metastases were compared to normal appearing white matter (NAWM) and glioblastoma (GBM) from a previous study. Comparisons were performed using either the Wilcoxon signed-rank test for paired comparisons or the Mann-Whitney nonparametric test for unpaired comparisons.

RESULTS: 49 patients with a primary histology of lung (n=25), breast (n=6), squamous cell carcinoma (SCC) (n=1), melanoma (n=5), gastrointestinal (GI) (n=3) and genitourinary (GU) (n=9) were included in comparison to GBM (n=31). The mean sRCBV of all metastases (1.83+/-1.05) were significantly lower (p=0.0009) than mean sRCBV for GBM (2.67$\pm$1.34) with both statistically greater (p<0.0001) than NAWM (0.68 +/- 0.18). Histologically distinct metastases are each statistically greater than NAWM (p<0.0001) with lung (p=0.0002) and GU (p=.02) sRCBV being significantly different than GBM sRCBV.

CONCLUSIONS: 49 patients with a primary histology of lung (n=25), breast (n=6), squamous cell carcinoma (SCC) (n=1), melanoma (n=5), gastrointestinal (GI) (n=3) and genitourinary (GU) (n=9) were included in comparison to GBM (n=31). The mean sRCBV of all metastases (1.83+/-1.05) were significantly lower (p=0.0009) than mean sRCBV for GBM (2.67$\pm$1.34) with both statistically greater (p<0.0001) than NAWM (0.68 +/- 0.18). Histologically distinct metastases are each statistically greater than NAWM (p<0.0001) with lung (p=0.0002) and GU (p=.02) sRCBV being significantly different than GBM sRCBV.

ABBREVIATIONS: dT1=delta T1; GBCA=gadolinium-based contrast agent; NAWM=normal appearing white matter; normalized relative cerebral blood volume=nRCBV; relative cerebral blood volume=rCBV; standardized relative cerebral blood volume=sRCBV

Received month day, year; accepted after revision month day, year.

From the Department of Biophysics (SKL, MAP, KMS), Medical College of Wisconsin, Milwaukee, WI, United States. From the Departments of Radiology (MJK, LSH), Mathematical Neuro-Oncology (JCU), Cancer Biology (LSU) and Neurological Surgery (LSU), Mayo Clinic, Phoenix, AZ, United States. From the Departments of Radiology (DP, MSS), Radiation Oncology (JY), Neurological Surgery (FJA) and Population and Public Health Sciences (MSS), Keck School of Medicine of University of Southern California, Los Angeles, California, United States. From the Imaging Genetics Center (MSS), University of Southern California Mark and Mary Stevens Neuroimaging and Informatics Institute, Marina del Rey, California, United States.

Disclosure of potential conflicts of interest:

Precision Oncology Insights (co-founder L.S.H.); Imaging Biometrics LLC (medical advisory board L.S.H., financial interest (L.S.H., K.M.S.); IQ-AI Ltd. (ownership interest (L.S.H., K.M.S.)); Prism Clinical Imaging (ownership interest K.M.S., board membership K.M.S.). The remaining authors have no conflicts of interest to disclose.

Please address correspondence to Kathleen M. Schmainda, PhD, Department of Biophysics, Medical College of Wisconsin, 8701 Watertown Plank Road, Milwaukee, WI, 53226, United States; kathleen@mcw.edu.

SUMMARY SECTION

PREVIOUS LITERATURE: The importance of obtaining perfusion-weighted MRI data, most commonly dynamic susceptibility contrast MRI (DSC-MRI) data, is being increasingly recognized for the evaluation of brain metastasis. However, a lack of consistency in brain tumor perfusion studies, attributable to a lack of standard protocol, has resulted in a wide range of rCBV values that are inconsistent and difficult to reproduce between studies. To overcome this limitation a consensus protocol has been developed and used for the current studies in treatment-naïve brain metastases.**KEY FINDINGS:** First steps towards establishing consensus-acquisition benchmark values for standardized rCBV in brain metastases has been accomplished. The sRCBV can be used to distinguish brain metastases from normal-appearing brain and are generally less than sRCBV for glioblastoma. **KNOWLEDGE ADVANCEMENT:** The results of this study should enable greater consistency and cross-site comparisons of sRCBV for the evaluation of both treated and untreated brain metastases.

INTRODUCTION

Brain metastases is the most common tumor of the central nervous system, and the incidence is on the rise. One estimate reports the annual number of identified cases in the United States to be 23,598.[1] Yet, additional clinical data suggest that over 100,000 patients develop brain metastases each year.[2] This substantial and rising disease burden is in part due to an overall increase of primary cancers, but also better systemic therapies that increase the probability of metastatic disease as the patients live longer[3]. The most common primary cancers are lung cancer, breast cancer and melanoma occurring in approximately 40-50%, 15-20% and 5-20% of patients newly diagnosed with brain metastases.[4] The average survival for patients with brain metastases is less than 6 months.[2]

Standard anatomic MRI, obtained with the administration of a gadolinium-based contrast agent (GBCA), is central to the diagnosis of brain metastases.[3] Yet, the importance of also obtaining perfusion-weighted MRI data, most commonly dynamic susceptibility contrast MRI (DSC-MRI) data, is being increasingly recognized. DSC-MRI, from which maps of relative cerebral blood volume (rCBV) can be generated, help to differentiate brain metastases from normal brain tissue and potentially distinguish brain metastases from primary brain tumors.[5] The use of rCBV has also been encouraged for distinguishing progressive tumor from pseudoprogession often due to post-treatment radiation effects[3], which often appear similar on post-contrast MRI.[6]

However, a lack of consistency in brain tumor perfusion studies, attributable to a lack of standard protocol, has resulted in a wide range of rCBV values that are inconsistent and difficult to reproduce between studies.[6] Likewise, as summarized in **Figure 1**, a wide range of MRI settings have been used for DSC-MRI studies in metastatic brain tumors[7–29], all of which affect the quality and accuracy of derived rCBV maps.[30] This variability may limit the ability of rCBV to identify metastases in distinction from normal brain and/or differentiate metastases

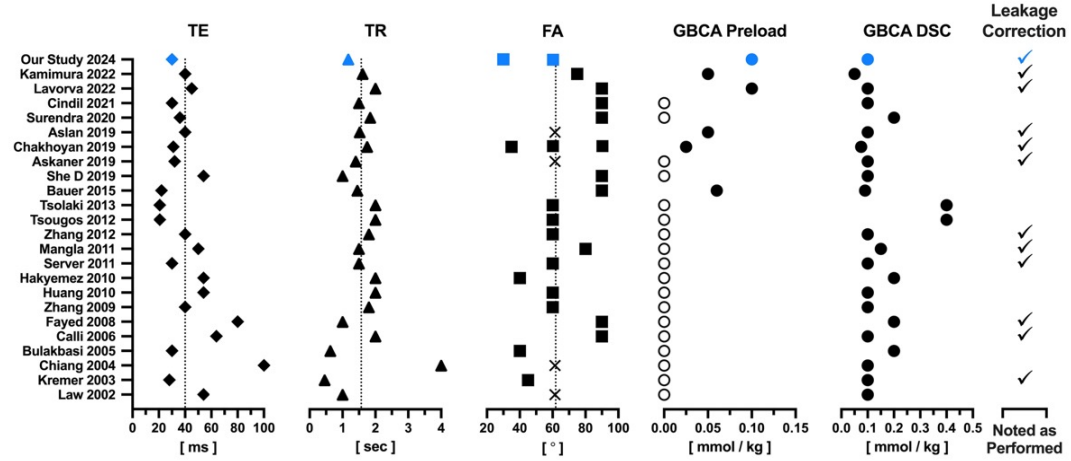

Figure 1. Summary of DSC-MRI parameter settings for studies that reported rCBV (relative cerebral blood volume) values for brain metastases. The studies were identified by performing a literature search using PubMed and Ovid Medline. The PubMed selection criteria used were "brain neoplasm*" OR "brain neoplasms" [MESH] OR "neoplasm metasta*" OR "brain metasta*") AND ("rCBV" or "relative cerebral blood")) AND ("DSCMRI" OR "DSC MRI" OR ("dynamic susceptibility contrast" AND ("magnetic resonance" OR "Magnetic Resonance Imaging" [MESH] OR "MRI"))) which yielded 248 publications. The Ovid Medline parameters used brain neoplasm, neoplasm metastases, brain metastases yielding 389714 publications. Further including cerebrovascular circulation or relative cerebral blood flow, DSCMRI or DSC MRI or dynamic susceptibility yielded 1240 publications. The inclusion of contrast and (magnetic resonance or MRI) yielded 313 publications. Limited further to English language and humans yielded 212 publications. With both Pubmed and Ovid Medline 23 studies resulted that reported an intratumoral rCBV value of brain metastases.[7-29] For these the DSC-MRI parameter settings are listed above along with the consensus settings used in the current study. Note the wide range in values used. The dashed line indicates median settings across all studies for TE (echo time), TR (repetition time), and FA (flip angle). Average values are shown for studies that reported a range of values, where unreported settings are designated with an X. Unfilled circles indicate studies for which a GBCA preload was not given. Mean values are shown when ranges were given. Settings used for our study are shown in blue. GBCA, gadolinium-based contrast agent.

from glioblastoma, for example. Pretreatment differentiation of these two most common intra-axial brain tumors is essential given the substantial difference in clinical workup and treatment strategies for each.[31] Consequently, while most studies suggest that the mean rCBV in brain metastases is less than glioblastoma given their well-characterized high vascularity[32], it is not surprising that the margin of difference ranges from negligible to significant. In response, a multi-investigator, multi-institutional working group was convened to formulate a national consensus recommendation for DSC-MRI data acquisition and post-processing[33]. This recommendation, initially developed for primary brain tumors, was also adopted for DSC-MRI of brain metastases.[3] Still, as Figure 1 confirms, this also means that benchmark rCBV values, determined with the consensus protocol, are lacking. It was therefore the goal of this study to establish rCBV benchmark values for metastatic brain tumors beginning with treatment-naive brain metastases. We hypothesize that the determination of benchmark rCBV values will enable the generalization of results that address questions of whether rCBV can be used to distinguish brain metastases from normal-appearing brain, or primary brain tumor and/or in distinction from metastases of different primary histology. To begin to address this goal, we chose to compute standardized rCBV (sRCBV)[34] as opposed to normalized rCBV (nRCBV), the latter of which requires the subjective determination of a normalizing reference ROI. For sRCBV, a predetermined calibration is used to generate quantitative sRCBV maps precluding the need for a reference ROI. Consequently, sRCBV provides more repeatable and consistent results across time and patients,[35,36] increasing the likelihood of distinguishing tissue types with threshold values that can be widely applied.

MATERIALS AND METHODS

Patients

All participants were enrolled in this HIPAA-compliant study according to the Institutional Review Board policy and approvals at each of three participating institutions (Medical College of Wisconsin, Mayo Clinic-Arizona, Keck School of Medicine of University of Southern California). Patients considered for inclusion were those with treatment-naive brain metastases who underwent an MRI exam that included DSC-MRI perfusion imaging. All diagnoses for metastases were confirmed surgically following biopsy or resection. Also included for comparison were participants from a single institution (Medical College of Wisconsin) who had histologically confirmed treatment-naive high-grade glioma with preoperative DSC-MRI.[37]

Imaging

All MRI exams were performed on 3.0 T MRI systems. Standard pre-contrast FLAIR and T1-weighted (T1w) spin-echo imaging were obtained according to the clinical protocol at each site with post-contrast T1w(T1+C) images obtained after administration of a 0.1mmol/kg dose of a GBCA. The pre- and post-contrast T1w images used the same acquisition parameters so that calibrated difference maps, referred to as delta T1 (dT1) maps, could be determined as previously described.[38] One of the two recommended consensus protocol options was used for all patients.[3,33] For this option the first GBCA dose (0.1mmol/kg) serves as a preload for the subsequent DSC-MRI data collection. Then, a 2nd GBCA dose (0.1 mmol/kg) is administered at 40-60sec during the acquisition of GRE-EPI images (FOV=220mm, matrix=96x96 or 128x128, slice thickness=4-5mm) using recommended parameter settings (FA=60º, TE/TR=30ms/1100-1250ms). The GRE-EPI data was collected for a total duration of 120s. When the DSC-MRI slices were not an exact subset of the T1-weighted slices, an additional T1-weighted "reference" scan was obtained using a slice prescription (orientation and spacing) matching the DSC-MRI exam for ease of co-registering the DSC-MRI images to the anatomic images.

Image and Statistical Analysis:

Standardized rCBV values were calculated on-site at each institution. This was made possible with the platform-independent IB Rad Tech™ plug-in (Imaging Biometrics LLC, Elm Grove, WI) available at each site. IB Rad Tech™ was used with either the Horos (https://horosproject.org) or OsiriX (https://www.osirix-viewer.com) dicom viewers. The customizable IB Rad Tech™ plug-in was designed to guide the user through the desired post-processing steps, most of which are automatic but allow user oversight. For this study these steps included registration of the T1w and DSC-MRI series, generation of dT1 maps[38], for delineation of contrast enhancing ROIs, and creation of standardized (calibrated) relative cerebral blood volume (sRCBV)[34] with leakage correction.[39] Specifically, first pre- and post-contrast T1weighted images are registered and individually standardized.[38] Next, delta T1 (dT1) maps are computed from the difference between the registered and standardized post- and pre-contrast T1-weighted images. The dT1 facilitate the visualization of the enhancing lesion, free of intrinsically increased T1 signal from blood products or proteinaceous material. Next, the user is prompted to draw a rough-bounding ROI around the enhancing lesion. Because dT1 maps are quantitative, a single, previously determined threshold is applied and an enhancing tumor ROI is generated.[38] Next, the T1w and DSC-MRI imaging series are registered and leakage-corrected, standardized (calibrated) relative cerebral blood volume (sRCBV)[34] generated.[39] Unlike normalized rCBV maps, standardized rCBV do not require user-drawn references ROIs for normalization. Mean sRCBV for metastases, using the dT1 ROIs (or T1+C ROIs when dT1 were not available), were determined and compared to sRCBV in untreated glioblastoma (GBM) from a previous study.[37] Mean sRCBV, from ROIs drawn within contralateral normal appearing white matter (NAWM) of each brain metastases patient, were also determined for purposes of comparison to normal-appearing brain tissue. The sRCBV for GBM and each group of metastases for a specific primary cancer were also compared to the NAWM from all metastases, a choice supported by the consistency of NAWM rCBV values when

standardized.[34] The Wilcoxon matched-pairs signed rank test was used to compare the metastases and NAWM sRCBV data as this is a paired dataset. For the remainder of comparisons, the Mann-Whitney nonparametric test was used. For both analyses a $p<.05$ was considered significant.

RESULTS

Forty nine patients, from three institutions (Medical College of Wisconsin =28, University of Southern California =12, Mayo Clinic Arizona = 9), with treatment naive brain metastases met inclusion criteria for this study. The pre-operative DSC-MRI studies took place between 11/21/2006 and 9/21/2020. The median age was 62 years with a range of 28-78 years. The patients included 23 males and 26 females. The primary histology for the brain metastases included lung (n= 25), squamous cell carcinoma (n=1), melanoma (n=5), gastrointestinal (GI) (n=3) and genitourinary (GU) (n=9). An additional 31 patients with histologically confirmed glioblastoma (according to the WHO 2016 classification[40]), who underwent pre-operative DSC-MRI from 2010 to 2014, were included for comparison. The glioblastoma data were included in a previously published report.[37]

An example MRI study with a corresponding sRCBV map is shown in **Figure 2** for a 64y male patient with primary lung cancer. The mean sRCBV for all

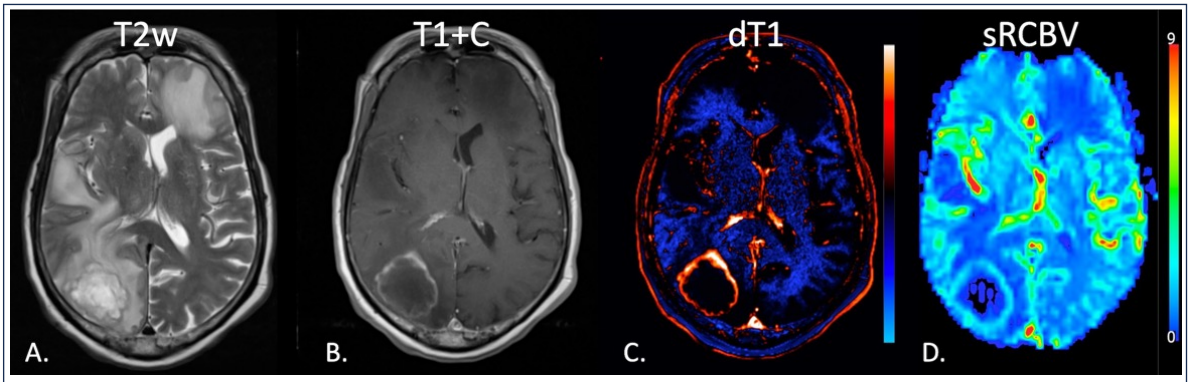

Figure 2. MRI study obtained in a 64y male patient with primary lung cancer. Shown are (A) a T2-weighted image, (B) post-contrast T1-weighted image, (C) delta T1 (dT1) map, and (D) corresponding standardized rCBV (sRCBV) map of one image slice showing the rim-enhancing brain metastasis. The mean sRCBV, for all lesions on all image slices, is 1.56 +/- 1.40.

metastases (1.83 +/- 1.05) is significantly lower ($p=.0009$) than the mean sRCBV for glioblastoma (2.67 +/- 1.34) with both statistically greater ($p<.0001$) than NAWM (0.68 +/- 0.18) (**Figure 3A**). The sRCBV for histologically-distinct metastases are also shown (**Figure 3B**) with each being statistically greater than NAWM ($p<.0001$) except for SCC which is non-evaluable given n=1. Lung ($p=0.0002$) and GU ($p=.02$) sRCBV were significantly less than GBM sRCBV while breast ($p=0.76$), melanoma ($p=0.86$) and GI ($p=0.41$) sRCBV were not. The individual sRCBV mean and standard deviation are as follows: lung (1.54 +/- 0.59), breast (2.28 +/-0.87), melanoma (2.48 +/- 1.24), GI (1.91 +/- 0.64) and GU (2.01 +/- 1.88).

DISCUSSION

By means of DSC-MRI perfusion imaging, which is consistent with the established consensus protocol for primary brain tumors[33] and incorporated for brain metastases[3], data obtained from three sites demonstrate that brain metastasis of different primary origins have sRCBV values that in general are significantly greater than NAWM, but significantly lower than sRCBV for glioblastoma. Unique to this study, sRCBV values of brain metastases were determined using the consensus DSC-MRI protocol.

The results of this study confirm that sRCBV should be helpful in identifying brain metastases as distinct from normal brain. These results reflect the fact that new vessel formation (ie angiogenesis) is a hallmark of brain metastases development.[41] Yet, given the reported variability in the degree of angiogenesis based on primary histology it was unclear that this result would apply to all metastases. Squamous cell carcinoma was the only metastatic type not showing

this distinction. But, with only two patients with SCC, a firm conclusion is not possible for this primary histology and a larger study is warranted.

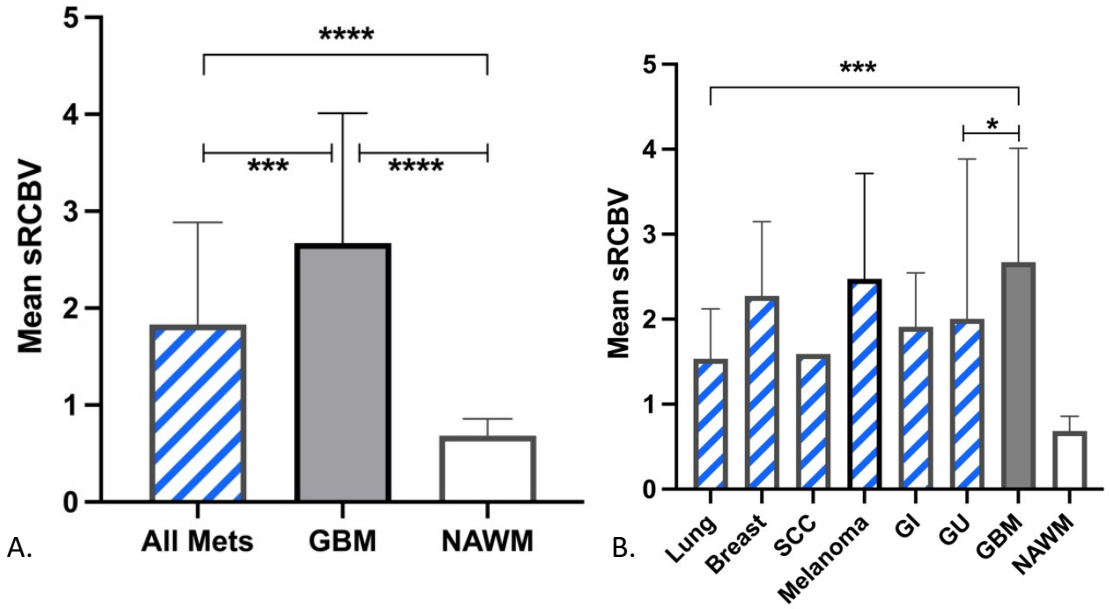

Figure 3. Mean standardized rCBV (sRCBV) (A) For all metastases (1.83 +/- 1.05) is statistically less than that for glioblastoma (GBM) (2.67 +/-1.34) (p=.0009) and significantly greater than the mean sRCBV for normal appearing white matter (NAWM) (0.68 +/- 0.18) (p<.0001). Likewise, mean sRCBV for GBM is statistically greater than for NAWM (p<.0001). (B). The sRCBV for histologically-distinct metastases are each statistically greater than NAWM (p<.0001), except for metastatic squamous cell carcinoma, which is non-evaluable with n=1. Lung (p<0.0001) and GU (p=.02) rCBV are also significantly different than GBM. The individual sRCBV mean, standard deviation and numbers (n) for each of histologically distinct brain metastases are lung (1.54 +/- 0.59, n=25), breast (2.28 +/-0.87, n=6), SCC (1.59, n=1), melanoma (2.48 +/- 1.24, n=5), GI (1.91 +/- 0.64, n=3) and GU (2.01 +/- 1.88, n=9) as compared to GBM (2.67 +/- 1.34, n=31) and NAWM (0.68 +/- 0.18, n=49).

Likewise, metastatic sRCBV was found to be less than glioblastoma sRCBV, a finding consistent with the well-known highly angiogenic nature of glioblastoma. However, the results were mixed when comparing individual metastases in comparison to glioblastoma. This is likely due to variations in angiogenesis for different metastatic types, but also to smaller numbers of patients for some categories. Even so, for all cases, metastatic mean sRCBV was less than glioblastoma mean sRCBV suggesting the possibility of distinction of untreated primary glioblastoma from metastatic tumor types based on sRCBV alone. While a recent study demonstrated that percent signal recovery (PSR), determined from the raw DSC signal, was better than rCBV for distinguishing lymphoma and primary and metastatic tumor types[26] these comparisons were performed using suboptimal DSC-MRI acquisition settings different from the national recommendation and did not include a comparison with standardized rCBV. Therefore, whether sRCBV or PSR is best for this distinction remains an open question. Alternatively, a combination of PSR and sRCBV can be used to provide the best distinction of these tumor types.

While all data in this study was collected with one of the two recommended acquisition options, previous studies have demonstrated the equivalence of these acquisition options for standardized rCBV.[42] Thus, we contend that comparable thresholds would likewise be determined if the single-dose low flip angle acquisition option were used. In addition to using the consensus recommendation for the acquisition of the perfusion MRI we also followed the recommendation to incorporate leakage correction as part of the post-processing.[33] Though a particular leakage correction algorithm was not specified as part of the consensus recommendation, we used one of the most common and well-published/proven approaches, referred to as the BSW leakage correction method.[39] As previously demonstrated, if rCBV maps are not corrected for leakage effects, their correlation with tumor aggressiveness is lost.[39,43] In addition, only when BSW leakage correction was applied did the single dose consensus option give results equivalent to the standard double dose option.[42]

Standardized rCBV (sRCBV) rather than normalized rCBV (nRCBV) was used in this study. The rationale is based on studies showing that sRCBV, while

providing information comparable to nRCBV, is more consistent than nRCBV, with lower coefficient of variation[34] and improved repeatability[35] across time-points. This greater consistency is due, at least in part, to the fact that sRCBV does not require the manual delineation of a reference ROI, which also makes possible the seamless and routine integration of automatic sRCBV map generation into the daily workflow. Furthermore, the fact that the standardization of rCBV results in a *quantitative* rCBV map has far reaching implications for the determination of thresholds to distinguish tissue and tumor types, which can be broadly applied. A recent example is the sRCBV thresholds determined to distinguish high-grade tumor from treatment effect.[44] This threshold is being used for the creation of fractional tumor burden (FTB) maps[45] with clinically-confirmed benefit to distinguish tumor progression from pseudoprogression.[28,46,47]

Several previous studies have likewise demonstrated that normalized rCBV is increased in primary brain tumors compared to brain metastases and NAWM.[11–13,15,17,21–23,29,48] However, there are large variations across sites, most likely due to differences in both the MRI acquisition protocols and post-processing methods used (See Figure 1.), making the data difficult to reproduce. This study uses data collected with the recently published consensus protocol together with one of the mostly widely used approaches for leakage correction thereby establishing a benchmark for all forthcoming studies seeking to use DSC-MRI for the evaluation of brain metastases.

As previously described it was possible for sRCBV to be calculated in the same way at each site using a customizable software plug-in available at each institution. The processing workflow can be customized according to the needs of each study or site, with respect to order of processing, types and names of input images and types of output parameter maps. Yet the core processing modules to create parameter maps, such as dT1 and sRCBV, remain fixed. This flexibility coupled with algorithmic consistency makes possible the widespread adoption and consistency of methodology and reported results across sites.

Study limitations include a small study population, with small numbers of patients in categories with less common metastases. Also, the focus was on untreated brain metastases only. However, the results motivate additional studies with more subjects, which may also help to address the possibility of making further distinctions among metastases resulting from different primary cancers. In addition, knowledge of untreated brain metastases is the first step towards addressing the utility of DSC-MRI for the evaluation of treated metastases. As with primary brain tumors, there is mounting evidence to indicate that rCBV can better distinguish tumor progression from non-tumor treated tissue than standard MRI alone.[6,44,49]

CONCLUSIONS

Using the consensus DSC-MRI acquisition protocol we have confirmed the utility of standardized rCBV to identify biologically active, treatment-naïve brain metastases as distinguished from normal appearing white matter and glioblastoma thus setting the benchmark for all subsequent studies adherent to the national consensus recommendation.

ACKNOWLEDGMENTS

Using the consensus DSC-MRI acquisition protocol we have confirmed the utility of standardized rCBV to identify biologically active, treatment-naïve brain metastases as distinguished from normal appearing white matter and glioblastoma thus setting the benchmark for all subsequent studies adherent to the national consensus recommendation.

REFERENCES

1. Cagney DN, Martin AM, Catalano PJ, et al. Incidence and prognosis of patients with brain metastases at diagnosis of systemic malignancy: A population-based study. *Neuro Oncol* 2017;19:1511–21.
2. Stelzer K. Epidemiology and prognosis of brain metastases. *Surg Neurol Int* 2013;4:S192-202.

3. Kaufmann TJ, Smits M, Boxerman J, et al. Consensus recommendations for a standardized brain tumor imaging protocol for clinical trials in brain metastases. *Neuro Oncol* 2020;22:757–72.

4. Eichler AF, Plotkin SR. Brain Metastases Opinion statement. *Curr Treat Options Neurol* 2008;10:308–14.

5. Derks SHAE, van der Veldt AAM, Smits M. Brain metastases: the role of clinical imaging. *British Journal of Radiology* 2022;95:20210944.

6. Patel P, Baradaran H, Delgado D, et al. MR perfusion-weighted imaging in the evaluation of high-grade gliomas after treatment: a systematic review and meta-analysis. *Neuro Oncol* 2017;19:118–27.

7. Law M, Cha S, Knopp EA, et al. High-grade gliomas and solitary metastases: differentiation by using perfusion and proton spectroscopic MR imaging. *Radiology* 2002;222:715–21.

8. Kremer S, Grand S, Berger F, et al. Dynamic contrast-enhanced MRI: differentiating melanoma and renal carcinoma metastases from high-grade astrocytomas and other metastases. *Neuroradiology* 2003;45:44–9.

9. Chiang IC, Kuo YT, Lu CY. Distinction between high-grade gliomas and solitary metastases using peritumoral 3T magnetic resonance spectroscopy, diffusion, and perfusion imaging. *Neuroradiology* 2004;46:619–27.

10. Bulakbasi N, Kocaoglu M, Farzaliyev A, et al. Assessment of diagnostic accuracy of perfusion MR imaging in primary and metastatic solitary malignant brain tumors. *American Journal of Neuroradiology* 2005;26:2187–99.

11. Calli C, Kitis O, Yunten N, et al. Perfusion and diffusion MR imaging in enhancing malignant cerebral tumors. *Eur J Radiol* 2006;58:394–403.

12. Fayed N, Dávila J, Medrano J, et al. Malignancy assessment of brain tumours with magnetic resonance spectroscopy and dynamic susceptibility contrast MRI. *Eur J Radiol* 2008;67:427–33.

13. Zhang H, Rödiger LA, Zhang G, et al. Differentiation between supratentorial single brain metastases and high grade astrocytic tumors: An evaluation of different DSC MRI measurements. *Neuroradiology Journal* 2009;22:369–77.

14. Huang BY, Kwock L, Castillo M, et al. Association of choline levels and tumor perfusion in brain metastases assessed with proton MR spectroscopy and dynamic susceptibility contrast-enhanced perfusion weighted MRI. *Technol Cancer Res Treat* 2010;9:327–37.

15. Hakyemez B, Erdogan C, Gokalp G, et al. Solitary metastases and high-grade gliomas: radiological differentiation by morphometric analysis and perfusion-weighted MRI. *Clin Radiol* 2010;65:15–20.

16. Server A, Orheim TED, Graff BA, et al. Diagnostic examination performance by using microvascular leakage, cerebral blood volume, and blood flow derived from 3-T dynamic susceptibility-weighted contrast-enhanced perfusion MR imaging in the differentiation of glioblastoma multiforme and brain metastasis. *Neuroradiology* 2011;53:319–30.

17. Mangla R, Kolar B, Zhu T, et al. Percentage signal recovery derived from MR dynamic susceptibility contrast imaging is useful to differentiate common enhancing malignant lesions of the brain. *AJNR Am J Neuroradiol* 2011;32:1004–10.

18. Zhang H, Zhang G, Oudkerk M. Brain metastases from different primary carcinomas: An evaluation of DSC MRI measurements. *Neuroradiology Journal* 2012;25:67–75.

19. Tsougos I, Svolos P, Kousi E, et al. Differentiation of glioblastoma multiforme from metastatic brain tumor using proton magnetic resonance spectroscopy, diffusion and perfusion metrics at 3 T. *Cancer Imaging* 2012;12:423–36.

20. Tsolaki E, Svolos P, Kousi E, et al. Automated differentiation of glioblastomas from intracranial metastases using 3T MR spectroscopic and perfusion data. *Int J Comput Assist Radiol Surg* 2013;8:751–61.

21. Bauer AH, Erly W, Moser FG, et al. Differentiation of solitary brain metastasis from glioblastoma multiforme: a predictive multiparametric approach using combined MR diffusion and perfusion. *Neuroradiology* 2015;57:697–703.

22. She D, Xing Z, Cao D. Differentiation of Glioblastoma and Solitary Brain Metastasis by Gradient of Relative Cerebral Blood Volume in the Peritumoral Brain Zone Derived from Dynamic Susceptibility Contrast Perfusion Magnetic Resonance Imaging. *J Comput Assist Tomogr* 2019;43:13–7.

23. Askaner K, Rydelius A, Engelholm S, et al. Differentiation between glioblastomas and brain metastases and regarding their primary site of malignancy using dynamic susceptibility contrast MRI at 3T. *Journal of Neuroradiology* 2019;46:367–72.

24. Chakhoyan A, Raymond C, Chen J, et al. Probabilistic independent component analysis of dynamic susceptibility contrast perfusion MRI in metastatic brain tumors. *Cancer Imaging* 2019;19:14.

25. Aslan K, Gunbey HP, Tomak L, et al. Multiparametric MRI in differentiating solitary brain metastasis from high-grade glioma: diagnostic value of the combined use of diffusion-weighted imaging, dynamic susceptibility contrast imaging, and magnetic resonance spectroscopy parameters. *Neurol Neurochir Pol* 2019;53:227–37.

26. Surendra KL, Patwari S, Agrawal S, et al. Percentage signal intensity recovery: A step ahead of rCBV in DSC MR perfusion imaging for the differentiation of common neoplasms of brain. *Indian J Cancer* 2020;57:36–43.

27. Cindil E, Sendur HN, Cerit MN, et al. Validation of combined use of DWI and percentage signal recovery-optimized protocol of DSC-MRI in differentiation of high-grade glioma, metastasis, and lymphoma. *Neuroradiology* 2021;63:331–42.

28. Lavrova A, Teunissen WHT, Warnert EAH, et al. Diagnostic Accuracy of Arterial Spin Labeling in Comparison With Dynamic Susceptibility Contrast-Enhanced Perfusion for Brain Tumor Surveillance at 3T MRI. *Front Oncol* 2022;12:849657.

29. Kamimura K, Nakajo M, Gohara M, et al. Differentiation of hemangioblastoma from brain metastasis using MR amide proton transfer imaging. *Journal of Neuroimaging* 2022;32:920–9.

30. Semmineh NB, Bell LC, Stokes AM, et al. Optimization of acquisition and analysis methods for clinical dynamic susceptibility contrast MRI using a population-based digital reference object. *American Journal of Neuroradiology* 2018;39:1981–8.

31. Kamimura K, Kamimura Y, Nakano T, et al. Differentiating brain metastasis from glioblastoma by time-dependent diffusion MRI. *Cancer Imaging* 2023;23.

32. Ahir BK, Engelhard HH, Lakka SS. Tumor Development and Angiogenesis in Adult Brain Tumor: Glioblastoma. *Mol Neurobiol* 2020;57.

33. Boxerman JL, Quarles CC, Hu LS, et al. Consensus Recommendations for a Dynamic Susceptibility Contrast MRI Protocol for Use in High-Grade Gliomas. *Neuro Oncol* 2020;22:1262–75.

34. Bedekar D, Jensen T, Schmainda KM. Standardization of relative cerebral blood volume (rCBV) image maps for ease of both inter- and intrapatient comparisons. *Magn Reson Med* 2010;64:907–13.

35. Prah MAA, Stufflebeam SMM, Paulson ESS, et al. Repeatability of standardized and normalized relative CBV in patients with newly diagnosed glioblastoma. *American Journal of Neuroradiology* 2015;36:1654–61.

36. Schmainda KM, Prah MA, Marques H, et al. Value of dynamic contrast perfusion MRI to predict early response to bevacizumab in newly diagnosed glioblastoma: results from ACRIN 6686 multicenter trial. *Neuro Oncol* 2021;23:314–23.

37. Schmainda KM, Prah MA, Rand SD, et al. Multisite concordance of DSC-MRI analysis for brain tumors: Results of a National Cancer Institute Quantitative Imaging Network Collaborative Project. *American Journal of Neuroradiology* 2018;39:1008–16.

38. Schmainda KM, Prah MA, Zhang Z, et al. Quantitative Delta T1 (dT1) as a replacement for adjudicated central reader analysis of contrast-enhancing tumor burden: A subanalysis of the American college of radiology imaging network 6677/radiation therapy oncology group 0625 multicenter brain tumor trial. *American Journal of Neuroradiology* 2019;40:1132–9.

39. Boxerman JLJL, Schmainda KMM, Weisskoff RMM. Relative cerebral blood volume maps corrected for contrast agent extravasation significantly correlate with glioma tumor grade, whereas uncorrected maps do not. *American Journal of Neuroradiology* 2006;27:859–67.

40. Whitfield BT, Huse JT. Classification of adult-type diffuse gliomas: Impact of the World Health Organization 2021 update. *Brain Pathology* 2022;32:e13062.

41. Berghoff AS, Preusser M. Anti-angiogenic therapies in brain metastases. *Memo - Magazine of European Medical Oncology* 2018;11.

42. Schmainda KM, Prah MA, Hu LS, et al. Moving toward a consensus DSC-MRI protocol: Validation of a low-flip angle single-dose option as a reference standard for brain tumors. *American Journal of Neuroradiology* 2019;40:626–33.

43. Donahue KMM, Krouwer HGJGJ, Rand SDD, et al. Utility of simultaneously acquired gradient-echo and spin-echo cerebral blood volume and morphology maps in brain tumor patients. *Magn Reson Med* 2000;43:845–53.

44. Prah MA, Al-Gizawiy MM, Mueller WM, et al. Spatial discrimination of glioblastoma and treatment effect with histologically-validated perfusion and diffusion magnetic resonance imaging metrics. *J Neurooncol* 2018;136:13–21.

45. Hoxworth JM, Eschbacher JM, Gonzales AC, et al. Performance of standardized relative CBV for quantifying regional histologic tumor burden in recurrent high-grade glioma: Comparison against normalized relative CBV using image-localized stereotactic biopsies. *American Journal of Neuroradiology* 2020;41:408–15.

46. Iv M, Liu X, Lavezo J, et al. Perfusion MRI-based fractional tumor burden differentiates between tumor and treatment effect in recurrent glioblastomas and informs clinical decision-making. *American Journal of Neuroradiology* 2019;40.

47. Connelly JM, Prah MA, Santos-Pinheiro F, et al. Magnetic Resonance Imaging Mapping of Brain Tumor Burden: Clinical Implications for Neurosurgical Management: Case Report. *Neurosurgery Open* 2021;2:2–5.

48. Skogen K, Schulz A, Dormagen JB, et al. Diagnostic performance of texture analysis on MRI in grading cerebral gliomas. *Eur J Radiol* 2016;85:824–9.

49. Hu LS, Eschbacher JM, Heiserman JE, et al. Reevaluating the imaging definition of tumor progression: perfusion MRI quantifies recurrent glioblastoma tumor fraction, pseudoprogression, and radiation necrosis to predict survival. *Neuro Oncol* 2012;14:919–30.